

Quantum Fluctuations of Chirality in One-Dimensional Spin- $\frac{1}{2}$ Multiferroics

Shunsuke Furukawa,¹ Masahiro Sato,¹ Yasuhiro Saiga,² and Shigeki Onoda¹

¹*Condensed Matter Theory Laboratory, RIKEN, Wako, Saitama 351-0198, Japan*

²*Department of Physics, Nagoya University, Nagoya 464-8602, Japan*

(Dated: September 29, 2019)

Properties of one-dimensional (1D) quantum multiferroics are revealed by means of exact diagonalization and bosonization of a frustrated spin- $\frac{1}{2}$ chain with a weak easy-plane anisotropy and a biquadratic Dzyaloshinskii-Moriya interaction. Quantum fluctuations appreciably reduce the chiral ordering amplitude from the classical value, leaving nearly collinear spin correlations in short-range scales. In-plane chirality dynamics involves gapless solitonic excitations, which can be experimentally verified in the dielectric response. We discuss the relevance to 1D multiferroic cuprates.

PACS numbers: 75.80.+q, 77.80.-e, 75.10.Pq, 75.40.Gb

When the chiral symmetry is spontaneously broken by magnetic interactions in Mott insulators, a ferroelectric polarization appears through the spin-orbit interaction. This new prototype of multiferroic behavior has recently been found in a helical magnet TbMnO₃ [1, 2], and attracted a great interest for both its fundamental importance and its potential application to an electrical control of spins [2]. This magnetoelectric coupling between the vector spin chirality and the polarization [3, 4, 5] is ubiquitous in Mott insulators [6]. In particular, one-dimensional (1D) spin- $\frac{1}{2}$ multiferroics including LiCuVO₄ [7] and LiCu₂O₂ [8, 9] have offered the simplest but intriguing laboratory.

The chiral ordering can be triggered by a geometrical frustration of spin exchange interactions. A simple 1D spin Hamiltonian, a minimal model for LiCuVO₄ [10],

$$\mathcal{H} = \sum_{n=1}^2 \sum_j J_n [\mathbf{S}_j \cdot \mathbf{S}_{j+n} + (\Delta - 1) S_j^z S_{j+n}^z], \quad (1)$$

contains a geometrical frustration when the second-neighbor exchange coupling J_2 is antiferromagnetic, i.e., $J_2 > 0$, irrespective of the sign of the nearest-neighbor J_1 . Here, \mathbf{S}_j represents the spin at the site j and $\Delta (\leq 1)$ is an easy-plane anisotropy allowed even for spin- $\frac{1}{2}$ systems. In the classical limit, this Hamiltonian exhibits the chiral ground state when $|J_1|/J_2 < 4$, having a nonzero expectation value $\kappa^z = \langle \mathcal{O}_\kappa^z \rangle$ of the vector spin chirality

$$\mathcal{O}_\kappa^\alpha \equiv (1/L) \sum_j (\mathbf{S}_j \times \mathbf{S}_{j+1})^\alpha, \quad \alpha = x, y, z. \quad (2)$$

In fact, spins are subject to quantum fluctuations, which are particularly pronounced for the spin- $\frac{1}{2}$ system. In the Heisenberg case $\Delta = 1$, the chiral order is smeared out and valence bond solids emerge [11, 12]. The existence of a chiral phase with an incommensurate (IC) gapless excitation has been shown at least for small Δ and $|J_1|/J_2$ [13, 14]. However, its fate in a realistic situation $\Delta \approx 1$ has not been clarified.

The importance of quantum fluctuations also suggests a nontrivial chirality dynamics. This may be probed from the dielectric functions $\varepsilon^{ii}(\omega)$, as recently measured for the spin-2 system RMnO₃ [15, 16], where a nontrivial

dynamics with a possible electromagnon [17] has been pointed out. It is naturally expected that the chirality fluctuates more strongly in the spin- $\frac{1}{2}$ chain, though the issue has not been studied before.

In this Letter, we present a quantum theory for 1D multiferroics from the frustrated spin- $\frac{1}{2}$ chain. It is shown that when $|J_1|/J_2$ is small, the chiral long-range order (LRO) survives in a realistic region near the $SU(2)$ -symmetric case. The ordering amplitude is appreciably suppressed, leading to only weakly helical spin correlations. The dynamics of the in-plane chirality \mathcal{O}_κ^z includes gapless solitonic excitations and a gapful spinon particle-hole continuum, while that of the out-of-plane chirality \mathcal{O}_κ^y involves a gapful electromagnon.

We first examine the ground-state phase diagram of the frustrated spin- $\frac{1}{2}$ XXZ chain, Eq. (1) with $J_2 > 0$, particularly in the case of small $|J_1|/J_2$. We perform a scaling analysis based on the bosonization in the decoupled-chain

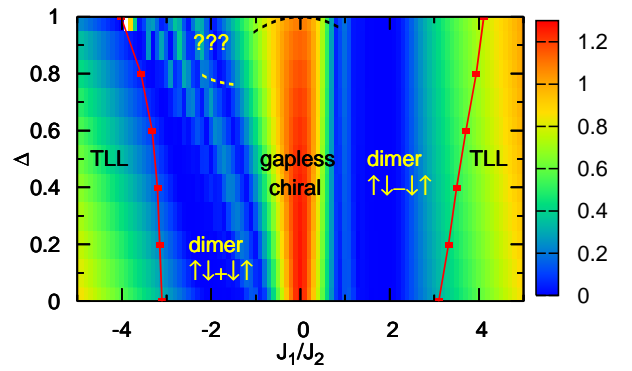


FIG. 1: (color online) Phase diagram of the spin- $\frac{1}{2}$ model (1), with the intensity plot of the Drude weight D_s/J_2 for $L = 28$ calculated by Lanczos diagonalization. The black broken line at $\Delta \approx 1$ shows a chiral phase boundary obtained in the scaling analysis. The yellow one at $\Delta \approx 0.8$ is a dimer phase boundary derived by the change of the ground-state sector for $L = 2 \times \text{odd}$. The red lines are the phase boundaries between TLLs and dimer phases determined in Refs. 18 and 19.

limit $J_1/J_2 \rightarrow 0$. When $|J_1| \ll J_2$, the low-energy effective Hamiltonian for Eq. (1) consists of two Tomonaga-Luttinger-liquid (TLL) parts $\mathcal{H}_\pm[\Phi_\pm, \Theta_\pm]$ and interaction terms \mathcal{H}_{int} , where (Φ_ν, Θ_ν) is the pair of dual boson fields defined in Ref. 13. The TLL parameters of the sectors \mathcal{H}_\pm are obtained as $K_\pm \approx K[1 \mp KJ_1\Delta a_0/(2\pi v) + O((J_1/J_2)^2)]$, where $K = (1 - \pi^{-1} \arccos \Delta)^{-1}$ and $v = (1 - \Delta^2)^{1/2}(2\pi^{-1} \arccos \Delta)^{-1} J_2 a_0$ are the TLL parameter and the spin-wave velocity for $J_1 = 0$, respectively, with a_0 being the lattice spacing. For the $SU(2)$ -symmetric case $\Delta = 1$ [11, 12], several marginally relevant terms in \mathcal{H}_{int} compete with each other, making it difficult to find what phases appear, especially, for $J_1 < 0$. However, an easy-plane anisotropy $\Delta < 1$ modifies their scaling dimensions. Then, two interaction terms $\mathcal{O}_c = (\partial\Theta_+) \sin(\sqrt{4\pi}\Theta_-)$ with the dimension $\Delta_c = 1 + 1/K_-$ and $\mathcal{O}_d = \cos(\sqrt{4\pi}\Phi_+) \cos(\sqrt{4\pi}\Theta_-)$ with the dimension $\Delta_d = K_+ + 1/K_-$ can be relevant for $J_1 > 0$, while only \mathcal{O}_c can for $J_1 < 0$. Here, a relevant $\mathcal{O}_{c(d)}$ can yield a gapless chiral (singlet-dimer) order. This scaling argument implies that when $J_1 > 0$, the phase boundary between dimer and chiral phases is fixed by the relation $\Delta_c = \Delta_d$ near the point $(\Delta, J_1/J_2) = (1, 0)$, and that when $J_1 < 0$, the chiral order appears under the condition $\Delta_c \leq 2$. Therefore, the phase boundary is derived as $\Delta \approx 1 - (J_1/J_2)^2/(2\pi^2) + \dots$ in the vicinity of $(\Delta, J_1/J_2) = (1, 0)$ irrespective of the sign of J_1 . Namely, a small easy-plane anisotropy, which is realistic for spin- $\frac{1}{2}$ systems, induces the chiral order. We also calculate the one-loop RG corrections to K_\pm , which suggest that the chiral phase is robust for $J_1 < 0$ while it is reduced by an expansion of the dimer phase for $J_1 > 0$.

The above bosonization prediction is supported by a numerical calculation of the spin Drude weight D_s , which reveals whether the spin excitation is gapless or gapped. We introduce a flux ϕ into the periodic chain, which transforms $S_j^\pm \rightarrow e^{\pm i\phi j/L} S_j^\pm$. The Drude weight D_s is given by the second derivative of the ground-state energy $E_{\text{GS}}(\phi)$ with respect to ϕ . To reduce finite-size effects, we average it [20] over $-\pi < \phi < \pi$, which leads to $D_s = \frac{L}{\pi} \frac{\partial^2 E_{\text{GS}}}{\partial \phi^2} |_{\phi=\pi-0}$. The result shown in Fig. 1 suggests that a gapless region extends from $\Delta = 0$ to 1 for small $|J_1|/J_2$, which can be identified with the gapless chiral phase. This region extends more largely on the ferromagnetic side $J_1 < 0$, in accordance with the one-loop RG analysis. Note that for small $1 - \Delta$ and $|J_1|/J_2$, the gap is extremely small if it exists and is difficult to detect in small-size calculations [12]. Thus, the actual phase boundaries should be curved downward as in the RG prediction. The region with small D_s for $J_1 > 0$ roughly corresponds to a gapped phase with a singlet-dimer on the nearest-neighbor bonds, though both chiral and dimer orders may coexist in a narrow region. In contrast, that for $J_1 < 0$ contains at least two phases: For small Δ , a dimer order appears [19] with a unit $|\uparrow\downarrow\rangle + |\downarrow\uparrow\rangle$ on the nearest-neighbor bonds, while for $\Delta \approx 1$, another

gapped phase is expected to appear [12]. The transition between these two phases is anticipated by a change of the ground-state sector from $\sigma_b = +1$ to $\sigma_b = -1$ in the eigenvalue of the inversion at the bond center, for $L = 2 \times \text{odd}$, which actually occurs around $\Delta \approx 0.8$ in our calculations. More precise determination of the phase diagram requires a further intensive study.

Now let us investigate properties of the chiral ground state, i.e., a quantum multiferroic. The uniform chirality κ^z produces the electric polarization P^y through the inverse DM interaction [3, 4, 5, 6] and generates the associated lattice modulation due to the electrostatic force. We take into account this coupling of spins to the transverse optical phonons through the DM interaction [21]. Integrating out the phonons gives a biquadratic DM interaction,

$$\mathcal{H}_{\text{spin-lat}} = -V_z \sum_j (\mathbf{S}_j \times \mathbf{S}_{j+1})^z (\mathbf{S}_{j+2} \times \mathbf{S}_{j+3})^z. \quad (3)$$

Here, longer-range terms have been neglected for simplicity. This term yields a gapless chiral order for quantum spin ladders [22] and a spin cholesteric (chiral nematic) for classical spin systems [21].

First, the chiral order parameter calculated from $\kappa^z = \sqrt{\langle (\mathcal{O}_\kappa^z)^2 \rangle}$ is shown in Fig. 2(a). The finite-size results are carefully extrapolated to $L \rightarrow \infty$ by the alternating ϵ -algorithm [23]. We take a small J_1/J_2 to assure that the system is inside the chiral phase even at $V_z = 0$ and to make the IC wave vector Q sufficiently close to $\pi/2$. Remarkably, when $V_z/J_2 \lesssim 2$ for $\Delta = 0.9$, κ^z is significantly suppressed from the classical value $S^2 = 1/4$, indicating appreciable quantum fluctuations of the chirality near the $SU(2)$ -symmetric case. This is consistent with the bosonization analysis combined with the mean-field theory [13], which gives $\kappa^z \sim |J_1/J_2|^{1/(K_- - 1)}$ with $K_- - 1 \sim \sqrt{1 - \Delta}$ near $\Delta = 1$. On the other hand, with increasing V_z , κ^z starts to increase rapidly around $V_z/J_2 \sim 2$ and approaches a constant $1/\pi$, which is the maximal value for the spin- $\frac{1}{2}$ case.

The weak chirality for $V_z/J_2 \lesssim 2$ has a remarkable consequence on the spin correlations. Figure 2 (b) shows the equal-time in-plane spin correlation, $\mathcal{S}^{+-}(q) = \langle S_q^+ S_{-q}^- \rangle$ with $S_q^\alpha = \sum_j S_j^\alpha e^{-iqj}/\sqrt{L}$ for $V_z/J_2 = 2$ and 4. To break the inversion symmetry in finite-size systems and to have a chiral order parameter comparable to the value extrapolated to $L \rightarrow \infty$ in Fig. 2(a), a flux $\phi = -0.8\pi$ is inserted as a mean field. While the result for $V_z/J_2 = 4$ (right panel) exhibits a single sharp peak at $q = Q \approx \pi/2$, that for $V_z/J_2 = 2$ (left panel) shows two comparable peaks at $q = \pm Q$ and a tiny asymmetry under the inversion $q \rightarrow -q$, reflecting a small chirality. According to the bosonization analysis, which reveals $\mathcal{S}^{+-}(Q) \rightarrow \infty$ due to a power-law spatial decay of this spin correlation [13], only the peak at $q = Q$ eventually diverges in the thermodynamic limit. The other peak at $q = -Q$ seen for

$V_z/J_2 = 2$ converges to a large but finite value. Nevertheless, except for the close vicinity of $q = \pm Q$, the asymmetry is small for $V_z/J_2 = 2$. Namely, when we introduce the collinear and helical (or spiral) components as $\mathcal{S}_{\parallel}(q) = \langle S_q^x S_{-q}^x + S_q^y S_{-q}^y \rangle = \frac{1}{2} [\mathcal{S}^{+-}(q) + \mathcal{S}^{+-}(-q)]$ and $\mathcal{C}_z(q) = \frac{1}{i} \langle (\mathbf{S}_q \times \mathbf{S}_{-q})^z \rangle = \frac{1}{2} [\mathcal{S}^{+-}(q) - \mathcal{S}^{+-}(-q)]$, respectively, the ratio $r(q) = \mathcal{S}_{\parallel}(q)/\mathcal{C}_z(q)$ converges to a rather small value, particularly for small V_z , except in the vicinity of $q = Q \sim \pi/2$ where it exactly becomes unity in the thermodynamic limit (see Fig. 2 (c)). Note that this quantity is related to the ratio α of the minor to major axes of elliptic spin correlations via $r = 2\alpha/(1 + \alpha^2)$. When $r = 0$ ($r = 1$), the spin correlation becomes collinear (a circular spiral). Therefore, the spin correlations are almost collinear at short-range scales and only the quasi-LRO component is characterized by a circular spiral with a pitch Q . This tendency is pronounced for a realistically small V_z . The helical to collinear crossover in the length scale also appears in the time scale. According to the bosonization analysis of the nearly $SU(2)$ -symmetric case, the dynamical structure factor $\mathcal{S}^{+-}(Q, \omega)$ diverges algebraically at the low-energy edge and only a tiny gap $\varepsilon_g \sim |J_1/J_2|^{K^-/(K^- - 1)}$ exists at $q = -Q$. Thus, dynamical spin correlations are *helical*

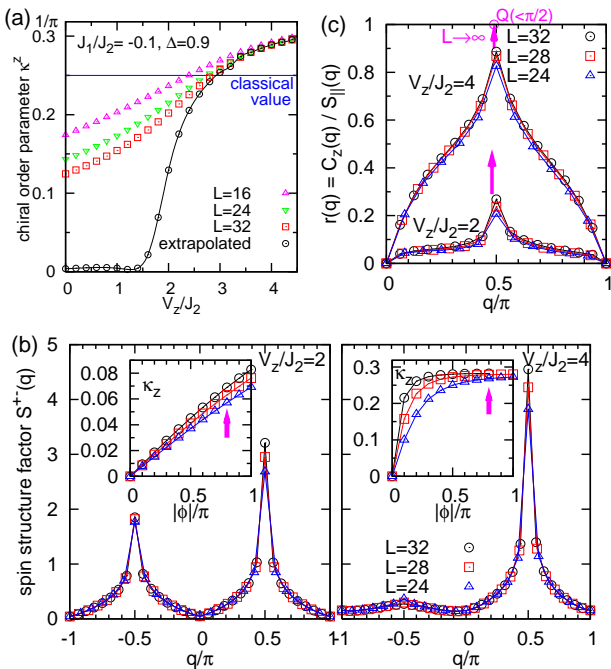


FIG. 2: (color online) (a) The chiral order parameter $\kappa^z = \sqrt{K^z}$ for $J_1/J_2 = -0.1$ and $\Delta = 0.9$ as a function of V_z/J_2 . Extrapolation is done from the sequence of data for $L = 16, 20, 24, 28$ and 32 , using the alternating ϵ -algorithm [23]. (b) The spin structure factor $\mathcal{S}^{+-}(q)$ for the same set of parameters and $V_z/J_2 = 2$ and 4 with a flux $\phi = -0.8\pi$. The insets show the ϕ -dependence of κ^z . (c) The ratio of the helical to collinear correlations.

only for $\omega, v||q| - Q| \lesssim \varepsilon_g$ and almost *collinear* otherwise.

This provides a key to understanding the puzzling results from a recent elastic polarized-neutron scattering experiment in LiCu_2O_2 [9]: $r(Q, 0) = \mathcal{C}_z(Q, 0)/\mathcal{S}_{\parallel}(Q, 0) \approx 20-40\%$ indicating an *elliptic* spiral, and $\mathcal{S}^{xx}(Q, 0) \approx \mathcal{S}^{yy}(Q, 0)$ indicating a *circular* spiral, if the observed elastic intensities are interpreted as the genuine Bragg peaks at $\omega = 0$ due to the 3D magnetic LRO. This problem can be resolved, at least qualitatively, if the fine but finite energy-momentum resolution allows an additional contribution from low-energy spin fluctuations to the elastic intensities. Actually, in our analysis of the gapless chiral phase, there exist large spin fluctuations outside the narrow window $\omega, v||q| - Q| \lesssim \varepsilon_g$, which show small r but retain $\mathcal{S}^{xx} = \mathcal{S}^{yy}$. Detailed inelastic polarized neutron scattering experiments are required to test this possibility and to reveal nontrivial effects of a weak 3D coupling on the spin dynamics.

Next, we discuss dynamical in-plane and out-of-plane chiral correlations, $K^z(\omega)$ and $K^y(\omega)$, respectively;

$$K^\alpha(\omega) = -\frac{L}{\pi} \Im \lim_{\eta \rightarrow 0^+} \langle \text{GS} | \mathcal{O}_\kappa^\alpha \frac{1}{\omega - \mathcal{H} + i\eta} \mathcal{O}_\kappa^\alpha | \text{GS} \rangle. \quad (4)$$

These spectra appear in dielectric functions $\varepsilon^{\alpha\beta}(\omega)$ through the magnetoelectric coupling $P^\alpha \propto \varepsilon_{\alpha\beta\gamma} \mathcal{O}_\kappa^\beta$ [6], where $\varepsilon_{\alpha\beta\gamma}$ is the Levi-Civita tensor. Hence we have $\Im \varepsilon^{yy}(\omega) \propto K^z(\omega)$ and $\Im \varepsilon^{zz}(\omega) \propto K^y(\omega)$. Figure 3 (a) shows the numerical continued-fraction analysis of Lanczos results for several L 's. In the insets, we clarify finite-size effects on the energy levels of the pseudo ground state (PG), the first and second excited states (A and B), and the higher-energy state (C) with large intensity. The same parameter values $(J_1/J_2, \Delta) = (-0.1, 0.9)$ as in Fig. 2 have been adopted. In the chiral ground state with $\kappa^z \propto P^y \neq 0$, the excitation via the state PG does not contribute to $K^z(\omega)$. Therefore, the level B gives the lowest-energy excitation gap in $K^z(\omega)$. Then, it is evident from the insets that $K^z(\omega)$ ($\propto \Im \varepsilon^{yy}$) eventually becomes gapless in the thermodynamic limit irrespective of the magnitude of V_z (and thus κ^z), even though the system is a Mott insulator. On the other hand, $K^y(\omega)$ ($\propto \Im \varepsilon^{zz}$), which corresponds to the channel of electromagnons [15, 16, 17], is clearly gapful for $V_z/J_2 = 3$. For $V_z/J_2 = 0$, it is difficult to reliably estimate the gap, since it should be very small.

Further insights on the chirality dynamics in the gapless chiral phase can be gained from the bosonization picture [13]. It represents the spin and the chirality as $S_{j=2n-1}^{2n} \sim e^{i\sqrt{\pi}(\Theta_{++} + (-)^n \Theta_-)} [(-1)^n c_1 + \dots]$ and $\mathcal{O}_\kappa^z \sim \mathcal{O}_\kappa^{z(1)} + c_2 \mathcal{O}_\kappa^{z(2)} + \dots$ with $\mathcal{O}_\kappa^{z(1)} = \int \frac{dx}{La_0} \sin(\sqrt{4\pi}\Theta_-)$ and $\mathcal{O}_\kappa^{z(2)} = \int \frac{dx}{La_0} \sin(\sqrt{4\pi}\Theta_-) \cos(\sqrt{4\pi}\Phi_+)$. Here, $c_{1,2}$ are constants of $O(1)$. The field Θ_- is locked to have the chiral LRO, and hence the \mathcal{H}_- sector has an excitation gap. The leading term $\mathcal{O}_\kappa^{z(1)}$ gives rise to a particle-hole continuum of spinons with the finite gap ε_g , which, in

our small-size calculations, may correspond to the shaded spectrum in $K^z(\omega)$ above the energy level C in Fig. 3 (a). Similarly, the bosonization reveals that the excitations in $K^y(\omega)$, which is mainly composed of a convolution of in-plane and out-of-plane spin excitations, has a finite gap $\sim \varepsilon_g$. As we mentioned above, the gap ε_g is rather small near the $SU(2)$ -symmetric case.

On the other hand, the subleading term $\mathcal{O}_\kappa^{z(2)}$ contains a gapless excitation because $\sin(\sqrt{4\pi}\Theta_-)$ has the LRO constant and the \mathcal{H}_+ sector is still described by a TLL in the chiral phase [13]. Therefore, $K^z(\omega)$ involves not only the gapped continuum but also a gapless mode, which may correspond to the spectrum from B . Note that $\cos(\sqrt{4\pi}\Phi_+)$ translates Θ_+ by $\sqrt{\pi}$. In other words, $\int dx \cos(\sqrt{4\pi}\Phi_+)$ coincides with the leading term

in the bosonized form of $\sum_j S_j^z S_{j+1}^z$, which rotates the two neighbouring spins by π about the z axis. Accordingly, the gapless excitation induced by $\mathcal{O}_\kappa^{z(2)}$ consists of two solitons, as schematically shown in Fig. 3 (c)-(e): An operation of $\mathcal{O}_\kappa^{z(2)}$ transforms a state from (c) to (d). It creates a pair of kinks with a negative (R) chirality in the positive (L) chiral background. Then, via the exchange of two neighbouring chiral spin pairs denoted by circles, the kinks propagate without changing the sign of the chirality of each domain, as shown in (e). This soliton appears through a chiral pairing of two spinons, in contrast to the conventional gapless spinon in 1D spin- $\frac{1}{2}$ antiferromagnets. If the $U(1)$ symmetry is weakly broken by spin anisotropies or by an in-plane magnetic field, the soliton can acquire a small gap. It will be interesting to look for this soliton by low-frequency optical probes.

In real materials, an inter-chain coupling J' causes the 3D helical LRO. However, a low transition temperature $T_N \approx 2K$ in LiCuVO_4 [7, 10] suggests that the effect of J' is small and should not alter our main conclusions.

The authors thank A. Furusaki, H. Katsura, N. Kida, T. Momoi, N. Nagaosa, S. Seki, Y. Tokura for stimulating discussions. The work was partly supported by Grant-in-Aids for Young Scientists (No. 19840053) from Japan Society for the Promotion of Science, and by Grant-in-Aid for Scientific Research (No. 17071011) and the 21st Century COE program ‘‘ORIMUM’’ at Nagoya Univ. from MEXT of Japan. The calculations were partly performed using supercomputers in ISSP, Univ. of Tokyo.

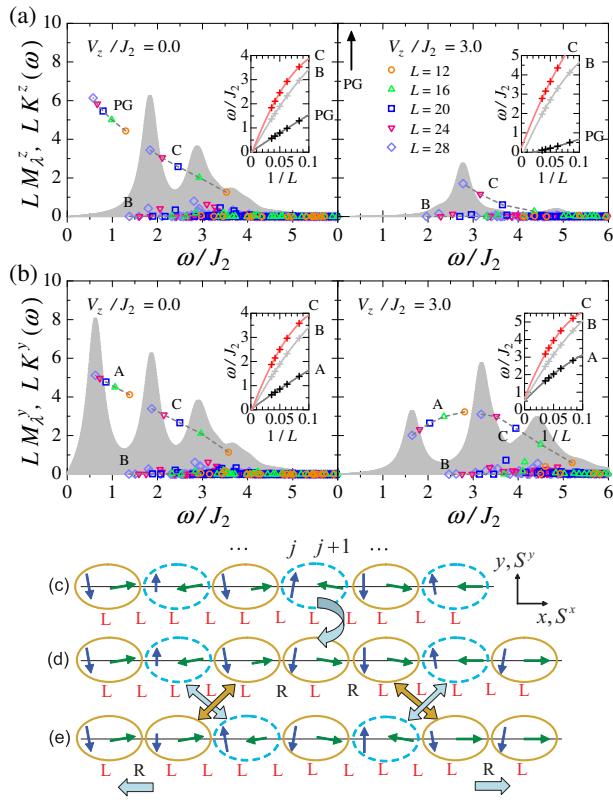


FIG. 3: (color online) Dynamical (a) in-plane and (b) out-of-plane chiral correlation functions, $K^z(\omega)$ and $K^y(\omega)$, respectively, for $J_1/J_2 = -0.1$, $\Delta = 0.9$, and $V_z/J_2 = 0$ and 3. The symbols show the matrix elements $LM_\alpha^\lambda = L^2 \langle \lambda | \mathcal{O}_\kappa^\lambda | \text{GS} \rangle^2$ at $\omega = \omega_\lambda$, where $|\lambda\rangle$ denotes an eigenstate with energy ω_λ measured from the (true) ground state. The shaded areas represent the spectra for $L = 28$ drawn with $\eta = 0.2J_2$ (see Eq. (4)). The insets show the extrapolations of the low-energy levels depicted as PG , A , B , and C into $L \rightarrow \infty$. In (a), $LM_{\lambda=PG}^z$ for $V_z/J_2 = 3$ take large values (13-50). (c-e) Schematic pictures on the creation and propagation of the chiral soliton pair. The symbol L (R) denotes a positive or left-handed (negative or right-handed) chirality at each bond.

- [1] T. Kimura *et al.*, *Nature* **426**, 55 (2003).
- [2] Y. Tokura, *Science* **312**, 1481 (2006); S.W. Cheong and M. Mostovoy, *Nature Materials* **6**, 12 (2007).
- [3] H. Katsura, N. Nagaosa, and A.V. Balatsky, *Phys. Rev. Lett.* **95**, 087205 (2005).
- [4] I.A. Sergienko and E. Dagotto, *Phys. Rev. B* **73**, 094434 (2006).
- [5] A.B. Harris *et al.*, *Phys. Rev. B* **73**, 184433 (2006).
- [6] C. Jia, S. Onoda, N. Nagaosa, and J.H. Han, *Phys. Rev. B* **74**, 224444 (2006); *Phys. Rev. B* **76**, 144424 (2007).
- [7] Y. Naito *et al.*, *J. Phys. Soc. Jpn.* **76**, 023708 (2007); Y. Yasui *et al.*, [arXiv:0711.1214](https://arxiv.org/abs/0711.1214); F. Schrettle *et al.*, [arXiv:0712.3583](https://arxiv.org/abs/0712.3583).
- [8] S. Park *et al.*, *Phys. Rev. Lett.* **98**, 057601 (2007).
- [9] S. Seki *et al.*, [arXiv:0801.2533](https://arxiv.org/abs/0801.2533).
- [10] M. Enderle *et al.*, *Europhys. Lett.* **70**, 237 (2005). Their neutron scattering results give $J_1 \sim -12K$ and $J_2 \sim 41K$.
- [11] S.R. White and I. Affleck, *Phys. Rev. B* **54**, 9862 (1996).
- [12] C. Itoi and S. Qin, *Phys. Rev. B* **63**, 224423 (2001).
- [13] A.A. Nersisyan, A.O. Gogolin, and F.H.L. Eßler, *Phys. Rev. Lett.* **81**, 910 (1998).
- [14] T. Hikihara, M. Kaburagi, and H. Kawamura, *Phys. Rev. B* **63**, 174430 (2001).
- [15] A. Pimenov *et al.*, *Nature Physics* **2**, 97 (2006).
- [16] N. Kida *et al.*, [arXiv:0711.2733](https://arxiv.org/abs/0711.2733).
- [17] H. Katsura, A.V. Balatsky, and N. Nagaosa, *Phys. Rev.*

- Lett. **98**, 027203 (2007).
- [18] K. Nomura and K. Okamoto, J. Phys. A **27**, 5773 (1994).
- [19] R. D. Somma and A. A. Aligia, Phys. Rev. B **64**, 024410 (2001).
- [20] D. Poilblanc, Phys. Rev. B **44**, 9562 (1991).
- [21] S. Onoda and N. Nagaosa, Phys. Rev. Lett. **99**, 027206 (2007).
- [22] M. Sato, Phys. Rev. B **76**, 054427 (2007).
- [23] C.J. Hamer and M.N. Barber, J. Phys. A: Math. Gen. **14** 2009 (1981).